FEBS Letters 581 (2007) 4783–4788

Active site closure facilitates juxtaposition of reactant atoms for initiation of catalysis by human dUTPase

Balázs Varga[a], Orsolya Barabás[a], Júlia Kovári[a], Judit Tóth[a], Éva Hunyadi-Gulyás[b], Éva Klement[b], Katalin F. Medzihradszky[b], Ferenc Tölgyesi[c], Judit Fidy[c,d], Beáta G. Vértessy[a,*]

[a] *Institute of Enzymology, Biological Research Center, Hungarian Academy of Sciences, Budapest, Hungary*
[b] *Proteomics Laboratory, Biological Research Center, Hungarian Academy of Sciences, Szeged, Hungary*
[c] *Institute of Biophysics and Radiation Biology, Semmelweis University, Budapest, Hungary*
[d] *MTA-SE Biophysics Research Group, Semmelweis University, Budapest, Hungary*

Received 13 July 2007; revised 26 August 2007; accepted 1 September 2007

Available online 12 September 2007

Edited by Peter Brzezinski

Abstract Human dUTPase, essential for DNA integrity, is an important survival factor for cancer cells. We determined the crystal structure of the enzyme:α,β-imino-dUTP:Mg complex and performed equilibrium binding experiments in solution. Ordering of the C-terminus upon the active site induces close juxtaposition of the incoming nucleophile attacker water oxygen and the α-phosphorus of the substrate, decreasing their distance below the van der Waals limit. Complex interactions of the C-terminus with both substrate and product were observed via a specifically designed tryptophan sensor, suitable for further detailed kinetic and ligand binding studies. Results explain the key functional role of the C-terminus.

Keywords: Initiation of catalysis; Tryptophan sensor; High-throughput screening for ligand binding; Enzyme mechanism; Flexible C-terminus

1. Introduction

The ubiquitous dUTPase enzyme keeps cellular dUTP/dTTP ratios at a low level to prevent uracil incorporation into DNA [1,2]. Lack of the enzyme overloads the capacity of base-excision repair leading to chromosome fragmentation and thymine less cell death. In human cancer cells, the enzyme was proposed to be an important survival factor desensitising tumours against drugs perturbing thymidylate metabolism [3,4]. High levels of the nuclear isoform of human dUTPase correlates with bad prognosis in several tumours [5,6]. Targeting dUTPase was therefore suggested as a promising approach in combination with drugs already in clinical use against thymidylate synthase and dihydrofolate reductase.

The human enzyme, like most dUTPases, is a homotrimer with three active sites constructed from five highly conserved motifs and located at subunit interfaces [7]. The flexible C-terminal segment, essential for activity [8,9], was proposed to close over the active site pocket upon substrate binding [7,10–12]. Due to its flexibility, just a few 3D structures could locate this critical segment and unfortunately, these structures did not represent the catalytically competent conformations of the nucleotide ligands, thereby excluding the possibility of mechanistic interpretations [7,10,13,14]. Lack of a robust expression system for any physiological isoform of the human enzyme impeded further progress and necessitated the present study.

We cloned the nuclear isoform of human dUTPase into a high-yield bacterial expression system. The crystal structure of the enzyme in complex with the non-hydrolysable substrate analogue α,β-iminodUTP:Mg was determined and allowed analysis of the full-length C-terminal segment. Solution studies by limited proteolysis and calorimetry were complemented by a novel construct with a highly sensitive tryptophan sensor within the C-terminus. Results suggest that the C-terminal segment may contribute to initiation of catalysis and, in contrast to the *Escherichia coli* enzyme, forms important interactions with both the substrate and the product. The Trp sensor construct is proposed to be used for high-throughput ligand binding assays necessary for drug optimisation.

2. Materials and methods

2.1. Cloning and mutagenesis

The cDNA encoding the nuclear isoform of human dUTPase (a kind gift from Bob Ladner [15]) was cloned into pET3a by conventional PCR amplification. The resulting DUT-N-pET-3a plasmid was subsequently recloned to obtain the N-terminally His-tagged dUTPase (His-DUT-N) wherein the Phe158Trp mutation was introduced by Quikchange (Stratagene) using adequate primers (cf. Supplementary). Cloning was checked by DNA sequencing on both strands. Protein was expressed and purified as described previously [11] also using the NiNTA protocol (Novagen) for the His-tagged constructs. Protein concentration was measured using the molar extinction coefficient calculated from the amino acid composition for the monomer

$\varepsilon_{280\ nm} = 10430\ M^{-1}\ cm^{-1}$ (or $15930\ M^{-1}\ cm^{-1}$, for Phe158Trp mutant).

Enzyme activity was measured according to [16]. Catalytic rate constants were determined to be $8 \pm 3\ s^{-1}$, with no observable change for wild-type His-tagged and Phe158Trp mutant His-tagged species.

Limited tryptic digestion was carried out at 25 °C, using 28 μM dUTPase concentration and 1:250 (w/w) trypsin:dUTPase ratio in 10 mM sodium-phosphate buffer, pH 7.5, containing 150 mM NaCl, 5 mM $MgCl_2$ and saturating concentrations of ligands, if present.

Differential scanning microcalorimetry was performed using a Microcal VP-DSC between 20 and 80 °C at a scan rate of 1 °C/min on 12 μM dUTPase sample in 20 mM TES, 0.3 M NaCl, 1 mM dithiothreitol, 5 mM $MgCl_2$, pH 7.5 buffer.

*Corresponding author. Present address: Institute of Enzymology, Karolina út 29, H-1113 Budapest, Hungary. Fax: +36 1 4665465.
E-mail address: vertessy@enzim.hu (B.G. Vértessy).

0014-5793/$32.00
doi:10.1016/j.febslet.2007.09.005

Isothermal titration calorimetry experiments were carried out at 20 °C on a Microcal VP-ITC instrument. 270 μM protein in 20 mM HEPES, 1 mM $MgCl_2$, 150 mM NaCl, pH 7.5 buffer was titrated with 3–16 μl aliquots from a stock solution of 2.2 mM α,β-iminodUTP.

Fluorimetric studies were carried out on a Jobin Yvon Spex Fluoromax-3 spectrofluorimeter at 20 °C, with excitation at 295 nm (slit 2 nm), emission between 300 and 450 nm (slit 5 nm). Phe158Trp mutant dUTPase at 1 μM in 20 mM Tris/HCl, 1 mM $MgCl_2$ and 150 mM NaCl, pH 7.5 buffer was measured and titrated by addition of 1–2 μl aliquots from concentrated stock nucleotide solutions.

Mass spectrometry. Data were collected on a MALDI-TOF mass spectrometer (Reflex III, Bruker, Bremen, Germany) (cf. [9,11] and Supplementary material).

N-terminal microsequencing was carried out using the pulsed-liquid phase sequencer ABI 471A of Applied Biosystems, Inc., USA as in [11].

Crystallization and crystallography. dUTPase (282 μM), 1.25 mM α,β-iminodUTP and 10 mM $MgCl_2$ in 10 mM Tris/HCl, 50 mM NaCl, and 0.1 mM TCEP, pH 7.0 buffer was mixed with reservoir solution containing 0.1 M Na–HEPES buffer, pH 7.5 and 18–20% PEG3350 to generate a rhombohedral crystal. Structure of the dUTPase:α,β-iminodUTP:Mg complex was solved by molecular replacement (MOLREP [17]) using a truncated model of the apodUTPase trimer [7] (PDB ID:1Q5U). Electron density for the C-terminal arm of molecule A was clearly visible already in the initial map. The other two subunits of the trimer showed very weak initial densities for residues 147–164. After building of the C-terminus of subunit A, the corresponding residues for molecule B were visualized, and repeated building and refinement steps provided satisfactory fits of these residues (B147–B164) to the observed density. However, the later residues are characterized with relatively high B-factors in the refined model (29.1–58.2, to be compared with the average temperature factor of 20.2 for the whole structure and with corresponding values of chain A: 11.6–29.1), arguing for substantially higher mobility of this C-terminal arm. The C-terminus of molecule C (C147–C164) was not possible to build, even in the final maps. We have to note, however, that water molecules 200–210 roughly trace this part of the C chain. Phe158 from the C monomer is well visible, suggesting that lack of residues C147–C164 was not due to cleavage or exclusion by crystal contacts, but rather originates in more pronounced flexibility. In the final refined structure, careful comparative investigations of crystal packing interactions did not reveal any significant differences around the three C-terminal regions, reinforcing the conclusion that the asymmetry in C-terminus localization is not due to artefacts but may indicate increased conformational freedom of this segment, cf. also similar results in the previously deposited liganded human dUTPase structure PDB ID:1Q5U. Coordinates and structure factor data have been deposited in the Protein Data Bank with accession code 2HQU. Figures were produced using Pymol [18].

3. Results and discussion

3.1. Three-dimensional structural analysis

The overall protein fold of the present structure (resolution 2.2 Å) agrees with earlier studies: three β-pleated monomers form an intricately organized homotrimer by C-terminal arm swapping (Fig. 1A). Novel features, previously not accessible, also emerge: (i) the full-length C-terminal region is visualized for two monomers and (ii) the structure contains an isosteric substrate analogue (α,β-imino-dUTP) in the catalytically competent *gauche* conformation, as well as Mg^{2+} (Fig. 1B) [13,14]. Mg^{2+} accommodation is provided by one oxygen from each of

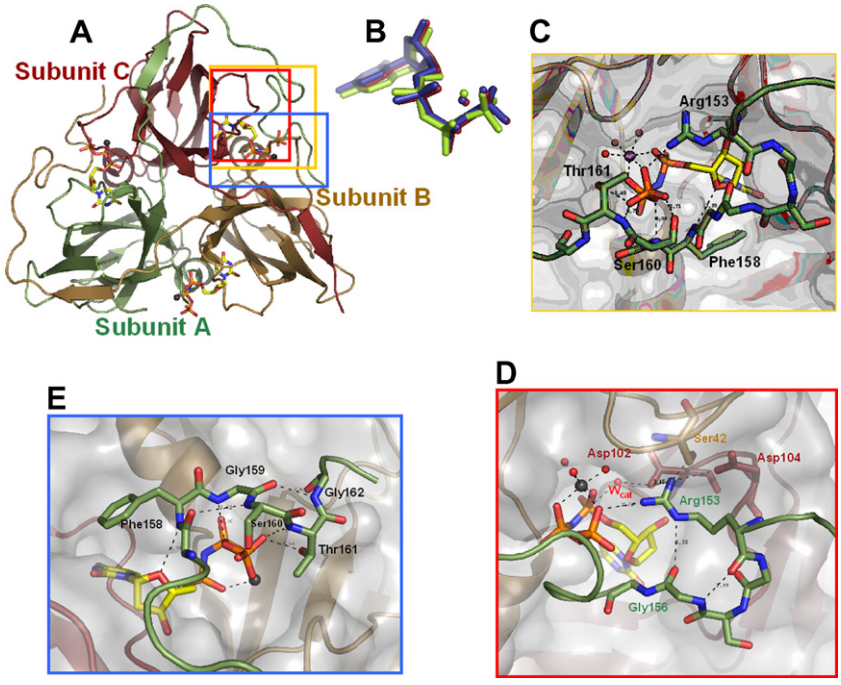

Fig. 1. 3D structure of the human dUTPase:α,β-iminodUTP:Mg complex. Colour-coded ribbon models of the subunits are presented with ligand molecules and Mg-ions shown in ball-and-stick model (yellow carbons and otherwise atomic colouring). (A) Overall 3D structure. Coloured rectangles indicate regions shown in detail on panels C–E. (B) Superimposed ligand molecules as bound in the active sites of the human dUTPase:α,β-iminodUTP:Mg (green), *Escherichia coli* dUTPase:α,β-iminodUTP:Mg (red) and inactive *E. coli* mutant dUTPase:dUTP:Mg (blue) complexes. Note that the phosphate chain conformation of the ligand in the presently determined structure presents the catalytically competent conformation [13]. (C) Interactions of the C-term tail with the ligand molecule. The C-terminal segment of monomer A is shown, with residues and ligand in ball-and-stick model. Ligand carbons are in yellow, protein carbons according to subunit colours, other atoms with atomic colouring. Rest of the protein is presented with ribbon model and transparent surface of the protein core. H-bonding interactions are in dashed lines. Note the extensive number of interactions formed between the C-terminus and the phosphate chain of the ligand that is in contrast to the limited number of interactions formed with the dUMP moiety. For panels (D) Close-up of the interactions formed by Arg153 and (E) β-turns accommodating the phosphate chain of the ligand, graphic representation as in panel C.

the three phosphate groups of the nucleotide and three water molecules, similar to the previous report on *E. coli* dUTPase [13]. Previously, only one structure visualized the entire C-terminus [10] and a single liganded human dUTPase structure was deposited [7]. Both lacked the nucleotide γ-phosphate group and the co-factor Mg^{2+} and represented mechanistically irrelevant ligand conformation (*trans* configuration of αP, unavailable for nucleophilic attack [13,14]), precluding true mechanistic insights.

Fig. 1C shows that only two interactions are present between the C-terminal tail and the dUMP moiety: (i) the Phe158 ring stacks over the uracil ring, and (ii) the Phe158 amide N H-bonds with the deoxyribose ring. In contrast, numerous contacts link the pyrophosphate leaving group to the C-terminus, suggesting its preferred localization upon substrate binding. Main chain atoms of residues 159–161 form H-bonds to the β- and γ-phosphates. Arg153 contributes to neutralization of the γ phosphate negative charge, in agreement with its essential role [9]. Arg153 also forms H-bonding with Ser42 of Motif 2 from the other subunit (Fig. 1D); this interaction helps to localize Arg153 to the core of the protein. The guanidino group approaches the main chain Gly156 O atom to form a small loop that may direct the flexible Arg side chain for functional interactions with the phosphates. An additional H-bond between Gly156 main chain N and Arg153 main chain O stabilizes this loop in a proper conformation (Fig. 1D).

For the first time, the role of the conserved Ser/Thr residues (Ser160 and Thr161), suggested to be of importance [12], can be analyzed (Fig. 1C). The hydroxyl groups of these residues form H-bonds with the two oxygen atoms of γ-phosphate not involved in chelating Mg^{2+}. Interestingly, Thr161 and Gly162 from one monomer also contact the side chains of Arg85 and Arg128, the conserved arginines from Motifs 2 and 4 from the neighbouring monomer involved in the active site. These interactions contribute to a fine-tuned charge distribution around the active site and also link the C-terminus of one monomer to residues in the other monomer within the core of the trimer. The Ser160N–Gly157O and Gly159O–Gly162N interactions shape two consecutive Type I turns for γ-phosphate accommodation (Fig. 1E).

The many contacts of the pyrophosphate group with the C-terminus are in contrast with its few interactions with the core of the trimer (H-bonding to an Arg85 side chain and to Gly87 main chain N). The Mg-ion is tightly bound to the phosphate chain, but contacts protein residues only indirectly via water molecules. These data may suggest that the pyrophosphate:Mg complex probably exits the active site with support from the flexible C-terminus.

Ordering of the C-terminal arms is not equivalent within the three monomers (Figs. 1A and 2): two of these arms are associated with appreciable electron densities (“closed” active sites), while the third cannot be localized. Similar asymmetry was already observed (PDB ID:1Q5U [7]). Detailed analysis of crystal packing interactions did not reveal any difference that may have resulted in this asymmetry. We interpret this result by assuming increased conformational freedom for the C-terminal residues. No significant alterations in conformation of active site residues or the nucleotide ligand could be observed when the three subunits were superimposed (Fig. 2D). However, the closed/open character of the active site is in clear correlation with the distance between the attacking nucleophile water oxygen and the substrate αP atom (2.77 and 2.79 vs. 3.23 Å) (Fig. 3). This correlation argues for a major role of arm-closure in facilitating approach of the reactant atoms

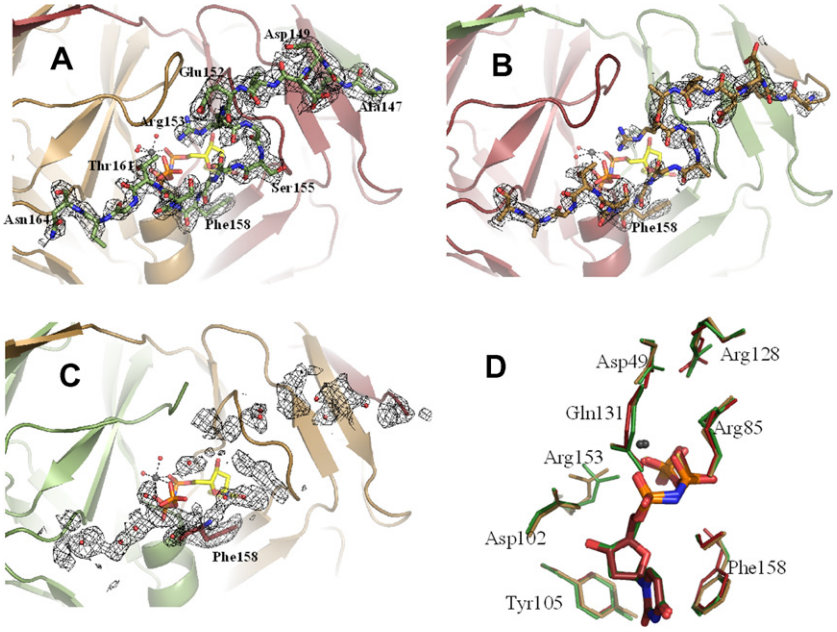

Fig. 2. Localization of the C-terminus (panels A–C) and superimposed active sites in the three subunits (panel D). Panels A, B, and C. 2Fo–Fc simulated annealed composite omit maps are shown at 0.8 sigma contour level for the C-terminal region (147–164) of the three subunits, displayed at the same orientation. Residues of the C-terminal arms are shown in ball-and-stick model while ribbon representation is used for the rest of the protein. For subunit “C”, water molecules approximately tracing the arm of molecule C are also shown as red balls (panel C). In panel A, some residues are labelled for orientation purposes. Panel D. The three subunits were superimposed using all atoms present in all the three monomers. Representative active site residues from the conserved motifs are shown together with the nucleotide ligand and magnesium. Residues are coloured according to subunits, nucleotides are shown with atomic colouring (carbon colour according to subunits, magnesium is gray).

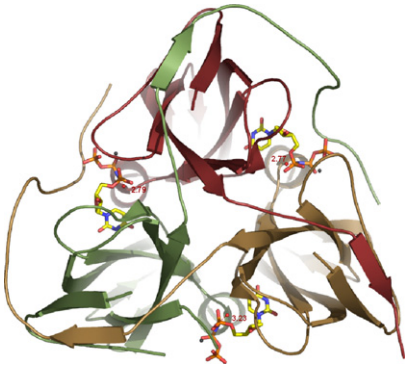

Fig. 3. Arm closure correlates to decreased distance between reactant atoms. Ligand molecules, Mg-ions and W_{cat} molecules are presented in ball-and-stick within the protein ribbon. Observe the correlation between arm closure and shortening of the αP–W_{cat} distance.

during catalysis. The sum of van der Waals radii for oxygen and phosphorus is 3.32 Å [19], i.e. significantly larger than observed in the closed active sites. Therefore, the present structure may represent a near-attack conformation approaching the intermediate of the reaction that is initiated by the nucleophilic attack of the incoming water oxygen atom on the αP [13]. No such observations could be made previously as structures lacked key components of the catalytically competent enzyme–substrate complex precluding identification of the nucleophile, and since the *gauche* conformation of the αP and the presence of the Mg^{2+} cofactor does not necessarily allow ordering of the C-terminal arm [20].

3.2. Conformational studies in solution

In order to check folding and stability of the recombinant protein, differential scanning calorimetry was applied [11,21,22]. Melting temperature was found to be 61.7 °C, closely similar to the value obtained for *Drosophila melanogaster* or *Plasmodium falciparum* dUTPases (56.5 °C and 63.8 °C, respectively) and considerably lower than for *E. coli* dUTPase (74.7 °C), indicating decreased stability of eukaryotic dUTPases [21,22]. Lower thermostability may be partially due to increased flexibility of N- and C-terminal segments. In fact, the N-terminus could not be localized in the 3D structure, and for one monomer, the C-terminus was also missing from the density maps. To analyze conformational shifts of these flexible segments possibly induced by substrate/product binding, limited proteolysis experiments were performed.

Limited proteolysis reaction mixtures revealed three tryptic sites (Fig. 4A). Masses at $MH^+ = 16131 \pm 3$ and 15181 ± 3, corresponding to fragments [16–164] and [16–153], respectively, appeared after 3 min of digestion. N-terminal microsequencing of these fragments confirmed cleavage site at Arg15 with ARPAE starting sequence. Cleavage at Arg15 was complete within 3–5 min of trypsinolysis and occurred even spontaneously in stock solutions, either in the absence or presence of nucleotides, suggesting that the N-terminal region is rather flexible and does not participate in nucleotide accommodation. On the contrary, binding of either α,β-imino-dUTP or dUMP exerted protection against cleavage at Arg153. Exclusively in the apo-enzyme, a third tryptic site was found at Arg44. This residue is located close to the nucleotide binding pocket; ligand binding may therefore induce a local subtle conformational change around this region resulting in protection against trypsinolysis.

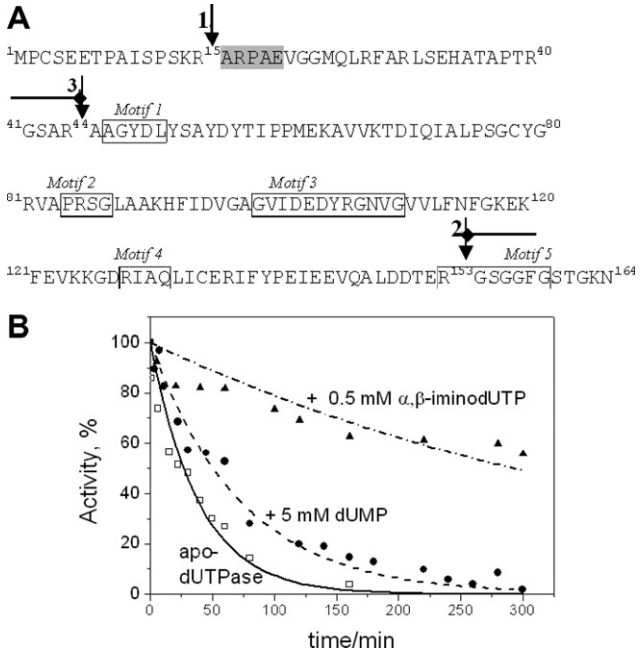

Fig. 4. Ligand-induced conformational changes followed by limited proteolysis. (A) Primary structure of human dUTPase (nuclear isoform). The His-tagged construct additionally contains the MGSSHHHHHHSSGLVPRGSH segment at the N-terminus. The three tryptic sites (in order of decreasing sensitivity: Arg15, Arg153, and Arg44) identified by mass spectrometry are marked with arrows. Block arrows at the sites Arg44 and Arg153 represent protection exerted by both α,β-iminodUTP and dUMP. The five highly conserved motifs are boxed. Grey background indicates five residues of the first two tryptic fragments (I and II) as identified by N-terminal microsequencing. (B) Time course of trypsinolysis followed by enzyme activity measurements. Graphs show loss of enzymatic activity due to an apparent first order reaction (cf. text and Supplementary material).

Enzymatic activity decrease during trypsinolysis followed an apparent first order reaction (with rate constants 0.0260, 0.0138, and 0.0023 min^{-1} for apodUTPase, dUTPase:dUMP, and dUTPase:α,β-iminodUTP complexes, respectively, cf. Fig. 4B and Supplementary Table II), in agreement with the rate estimated from MS results for cleavage at Arg153. Remaining activity is in good correlation with the amount of fragment [16–164] (data not shown), indicating the C-terminus is essential for activity (cf. [8,9]). The more pronounced protective effect of the substrate analogue suggests a different conformation of this region for the enzyme–substrate analogue as compared to the enzyme–product complex.

3.3. Equilibrium binding studies

Dissociation constant of the dUTPase:α,β-iminodUTP complex was determined to be 7.2 μM by titration calorimetry (Fig. 5A), considerably lower than for homologous enzymes [8,9]. Stoichiometry data (around 0.6) indicated potential protein destabilisation during the lengthy calorimetric experiment. In order to design a fast and sensitive assay for ligand binding to the active site pocket, we mutated the Phe158 residue to Trp, and thus obtained a highly sensitive fluorescent label within the C-terminus, with no apparent change in k_{cat}. Ligand binding induced quenching of Trp fluorescence allowed deter-

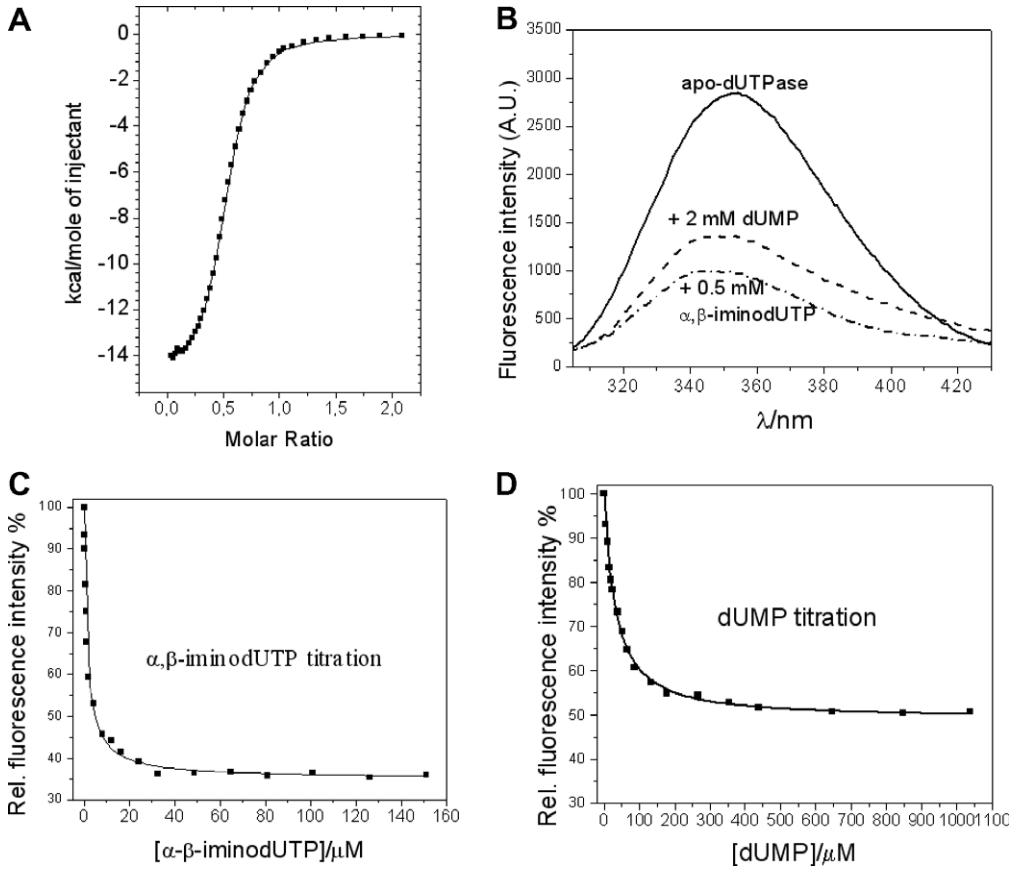

Fig. 5. Equilibrium ligand binding followed by isothermal titration calorimetry (A) and fluorimetry (B–D). (A) Data were fitted to "one type of sites" model using the MicroCal program. (B) Fluorescent spectra of unliganded dUTPase (straight line), dUTPase:α,β-imino-dUTP complex (dashed line) and dUTPase:dUMP complex (dash dotted line) (C, D) Relative fluorescent intensity data were fitted to the simplest model of 1:1 stoichiometry (see [8] for equation).

mination of K_d values (1.6 ± 0.2 μM for α,β-iminodUTP and 26.3 ± 2.8 μM for dUMP), with 1:1 stoichiometry for each subunit (Fig. 5B–D). Trp quenching is significantly larger in the enzyme:α,β-iminodUTP complex, arguing for different C-terminus conformations in the two nucleotide binding states, in agreement with trypsinolysis results. Binding strength of the substrate analogue to the human enzyme is very similar to the *E. coli* protein, but product binding is much stronger in the human enzyme than in the bacterial protein (cf. Supplementary Table III).

4. Conclusions

The 3D crystal structure reveals the coordinating role of the conserved C-terminal arm with high reliability and in-depth details. Flexibility of the C-terminus was different in the three active sites of the enzyme allowing comparison of closed and open active sites in the same homotrimer and suggesting a role for ordering of the C-terminus in facilitating approach of the reactant atoms. The Trp label in the C-terminal segment is proposed to be exploited in detailed mechanistic studies and for fast and quantitative screens for ligand binding to the active site region of human dUTPase.

Acknowledgements: We gratefully thank Bob Ladner at University of New Jersey for the cDNA of human dUTPase, and beamlines and operators at EMBL/DESY, Hamburg for assistance. This work was supported by Grants from Hungarian Scientific Research Fund (K68229), Howard Hughes Medical Institutes (#55005628 and #55000342), Alexander von Humboldt Foundation, Varga József Foundation (B.V.), Hungarian Economic Competitiveness Operative Programme GVOP-3.2.1.-2004-05-0412/3.0, FP6 STREP 012127 and FP6 SPINE2c LSHG-CT-2006-031220, and EMBO Long-Term Fellowship to J.T.

Appendix A. Supplementary data

Supplementary data associated with this article can be found, in the online version, at doi:10.1016/j.febslet.2007.09.005.

References

[1] Shlomai, J. and Kornberg, A. (1978) Deoxyuridine triphosphatase of *Escherichia coli*. Purification, properties, and use as a reagent to reduce uracil incorporation into DNA. J. Biol. Chem. 253, 3305–3312.
[2] Pearl, L.H. and Savva, R. (1996) The problem with pyrimidines. Nat. Struct. Biol. 3, 485–487.
[3] Pugacheva, E.N., Ivanov, A.V., Kravchenko, J.E., Kopnin, B.P., Levine, A.J. and Chumakov, P.M. (2002) Novel gain of function activity of p53 mutants: activation of the dUTPase gene expression leading to resistance to 5-fluorouracil. Oncogene 21, 4595–4600.

[4] Chano, T. et al. (2004) Differentially expressed genes in multidrug resistant variants of U-2 OS human osteosarcoma cells. Oncol. Rep. 11, 1257–1263.
[5] Romeike, B.F., Bockeler, A., Kremmer, E., Sommer, P., Krick, C. and Grasser, F. (2005) Immunohistochemical detection of dUTPase in intracranial tumors. Pathol. Res. Pract. 201, 727–732.
[6] Ladner, R.D., Lynch, F.J., Groshen, S., Xiong, Y.P., Sherrod, A., Caradonna, S.J., Stoehlmacher, J. and Lenz, H.J. (2000) dUTP nucleotidohydrolase isoform expression in normal and neoplastic tissues: association with survival and response to 5-fluorouracil in colorectal cancer. Cancer Res. 60, 3493–3503.
[7] Mol, C.D., Harris, J.M., McIntosh, E.M. and Tainer, J.A. (1996) Human dUTP pyrophosphatase: uracil recognition by a beta hairpin and active sites formed by three separate subunits. Structure 4, 1077–1092.
[8] Vertessy, B.G., Larsson, G., Persson, T., Bergman, A.C., Persson, R. and Nyman, P.O. (1998) The complete triphosphate moiety of non-hydrolyzable substrate analogues is required for a conformational shift of the flexible C-terminus in *E. coli* dUTP pyrophosphatase. FEBS Lett. 421, 83–88.
[9] Nemeth-Pongracz, V. et al. (2007) Flexible segments modulate co-folding of dUTPase and nucleocapsid proteins. Nucleic Acids Res. 35, 495–505.
[10] Prasad, G.S., Stura, E.A., Elder, J.H. and Stout, C.D. (2000) Structures of feline immunodeficiency virus dUTP pyrophosphatase and its nucleotide complexes in three crystal forms. Acta Crystallogr. D Biol. Crystallogr. 56, 1100–1109.
[11] Kovari, J. et al. (2004) Altered active site flexibility and a structural metal-binding site in eukaryotic dUTPase: kinetic characterization, folding, and crystallographic studies of the homotrimeric Drosophila enzyme. J. Biol. Chem. 279, 17932–17944.
[12] Dubrovay, Z., Gaspari, Z., Hunyadi-Gulyas, E., Medzihradszky, K.F., Perczel, A. and Vertessy, B.G. (2004) Multidimensional NMR identifies the conformational shift essential for catalytic competence in the 60-kDa *Drosophila melanogaster* dUTPase trimer. J. Biol. Chem. 279, 17945–17950.
[13] Barabas, O., Pongracz, V., Kovari, J., Wilmanns, M. and Vertessy, B.G. (2004) Structural insights into the catalytic mechanism of phosphate ester hydrolysis by dUTPase. J. Biol. Chem. 279, 42907–42915.
[14] Kovári, J., Barabás, O., Varga, B., Békési, A., Tölgyesi, F., Fidy, J., Nagy, J., Vertessy, B.G. (in press) Methylene substitution at the α–β bridging position within the phosphate chain of dUDP profoundly perturbs ligand accommodation into the dUTPase active site. Proteins.
[15] Ladner, R.D., McNulty, D.E., Carr, S.A., Roberts, G.D. and Caradonna, S.J. (1996) Characterization of distinct nuclear and mitochondrial forms of human deoxyuridine triphosphate nucleotidohydrolase. J. Biol. Chem. 271, 7745–7751.
[16] Vertessy, B.G. (1997) Flexible glycine rich motif of Escherichia coli deoxyuridine triphosphate nucleotidohydrolase is important for functional but not for structural integrity of the enzyme. Proteins 28, 568–579.
[17] Vagin, A. and Teplyakov, A. (1997) MOLREP: an automated program for molecular replacement. J. Appl. Crystallogr. 30, 1022–1025.
[18] DeLano, W.L. (2002) Pymol, DeLano Scientific, San Carlos, CA, USA.
[19] Bondi, A. (1964) J. Phys. Chem. 68, 441.
[20] Samal, A., Schormann, N., Cook, W.J., DeLucas, L.J. and Chattopadhyay, D. (2007) Structures of vaccinia virus dUTPase and its nucleotide complexes. Acta Crystallogr. D Biol. Crystallogr. 63, 571–580.
[21] Takacs, E., Grolmusz, V.K. and Vertessy, B.G. (2004) A tradeoff between protein stability and conformational mobility in homotrimeric dUTPases. FEBS Lett. 566, 48–54.
[22] Quesada-Soriano, I., Musso-Buendia, J.A., Tellez-Sanz, R., Ruiz-Perez, L.M., Baron, C., Gonzalez-Pacanowska, D. and Garcia-Fuentes, L. (2007) *Plasmodium falciparum* dUTPase: studies on protein stability and binding of deoxyuridine derivatives. Biochim. Biophys. Acta 1774, 936–945.